

Reproducibility and accuracy of LGE-CMR measurements related to detection of left atrial fibrosis in patients undergoing atrial fibrillation ablation procedures.

Andrei D Mărgulescu^{a,b}, Marta Nuñez-Garcia^c, Francisco Alàrcon^a, Eva M Benito^a, Norihiro Enomoto^a, Jennifer Cozzari^a, Fredy Chipa Ccasani^a, Hael Fernandez^a, Roger Borrás^a, Eduard Guasch^{a,d}, Constantine Butakoff^c, Oscar Camara^c, Lluís Mont Girbau^{a,d}

Running title: Reproducibility of LGE-CMR measurements in AF

- a. Cardiovascular Clinical Institute, UFA (Unitat de Fibril·lació Auricular de l'Hospital Clínic), Hospital Clínic, Universitat de Barcelona, IDIBAPS (Institut d'Investigació Biomèdica August Pi i Sunyer), Barcelona, Spain;
- b. Department of Cardiology, Morriston Cardiac Centre, Morriston Hospital, Heol Maes Eglwys, Morriston, Swansea, SA6 6NL, United Kingdom;
- c. Physense, Department of Information and Communication Technologies, Universitat Pompeu Fabra, Barcelona, Spain;
- d. CIBERCV (Centro de Investigación Biomédica en Red Cardiovascular), Barcelona, Spain.

Authors email addresses:

andrei_marg@yahoo.com; marta.nunez@upf.edu; falarcon@clinic.cat;
Benitom@clinic.cat; norihi_enomo@hotmail.com; jennifercozzari@gmail.com;
fredy_chipa@hotmail.com; hafernand@hotmail.com; Rborras@clinic.cat;
eguasch@clinic.cat; cbutakoff@gmail.com; oscar.camara@upf.edu; Lmont@clinic.cat

Corresponding author:

Dr. J. Lluís Mont Girbau

lmont@clinic.cat

Cardiology Department, Hospital Clinic

C/ Villarroel Nº 170. 08036 Barcelona

Tel: (+34) 932275551; Fax: (+34) 934513045

Conflicts of interest: Dr Lluís Mont is consultant, lecturer, and has received research funding from Biosense Webster, Boston Scientific, Medtronic, and St Jude Medical. He also has stock options of Galgo Medical.

The other authors have no relevant conflict of interest to declare.

Word count: 4210

Funding:

This work was partially supported by Fondo de Investigaciones Sanitarias-Instituto de Salud Carlos III (PI16/00435); Agencia de gestió d'Ajuts Universitaris i de Recerca (AGAUR, 2017SGR1548); CERCA programme/Generalitat de Catalunya; the European Union's Horizon 2020 research and innovation programme under grant agreement No 633196 (CATCH ME); the Spanish Ministry of Economy and Competitiveness (DPI2015-71640-R) and by the “Fundació La Marató de TV3” (nº 20154031).

Abstract

Objectives. To assess the intra- and inter-observer reproducibility and agreement of late-gadolinium-enhancement cardiac magnetic resonance (LGE-CMR) parameters with direct application to atrial fibrillation (AF) ablation techniques.

Background. LGE-CMR has been recently proposed to characterize left atrial (LA) anatomy and structural remodeling, and may facilitate AF ablation. For clinical application, a thorough description of the intra- and inter-observer reproducibility and agreement of LGE-CMR measurements is needed.

Methods. One experienced and 1 non-experienced observer performed complete LGE-CMR data analysis, twice, in 40 randomly selected LGE-CMR examinations (20 pre- and 20 post-ablation). In addition, 2 other experienced and 2 other non-experienced observers performed complete LGE-CMR data analysis in a subgroup of 30 patients (15 pre- and 15 post-ablation LGE-CMR) once.

Results. Both intra- and inter-observer reproducibility of LA volume, LA area, and Sphericity Index (SI) were good (Coefficients of variation, CV <10%, intra-class correlation coefficient, ICC >0.71). The geometric congruency of repeated reconstruction of LA shape was high, with maximal error <5mm for intra-observer and <8mm for inter-observer repeated measurements. The precision of scar location increased with extent of scar, and was high (Dice coefficient >0.75) when the scar area was >5cm² for a single observer, and >15 cm² for multiple observers. Non-experienced observers performed equally well to experienced observers.

Conclusions. LGE-CMR measurements of LA area, volume, SI are highly reproducible, and the geometric congruency of repeated reconstruction of LA shape is high. Location of scar is highly precise for scar areas >5cm² for single observers and

>15 cm² for multiple observers. LGE-CMR assessment of LA measurements and scar extension may be applied in clinical practice after minimal training.

Key words: reproducibility, cardiac magnetic resonance, atrial fibrosis, atrial fibrillation, ablation.

Condensed abstract.

Late-gadolinium-enhancement cardiac magnetic resonance (LGE-CMR) may characterize left atrial (LA) anatomy and structural remodeling, potentially facilitating atrial fibrillation (AF) ablation. We assessed the intra- and inter-observer reproducibility and agreement of LGE-CMR parameters with direct application to AF ablation. Measurements of LA size and shape (area, volume, sphericity index) were highly reproducible. The precision of scar location was high (Dice coefficient >0.75) when the scar area was $>5\text{cm}^2$ (intra-observer), and $>15\text{ cm}^2$ (inter-observer). Non-experienced observers performed equally well to experienced observers. LGE-CMR assessment of LA measurements and scar extension may be applied in clinical practice after minimal training.

Abbreviations.

AF, atrial fibrillation

CV, coefficient of variation

ICC, intra-class correlation coefficient

LGE-CMR, late-gadolinium-enhancement cardiac magnetic resonance

LA, left atrium

LAA, left atrial appendage

MV, mitral valve

PVI, pulmonary vein isolation

SI, sphericity index

Introduction.

Catheter ablation of atrial fibrillation (AF) resistant to pharmacological therapy has gained widespread use in the last 20 years (1). Pulmonary vein isolation (PVI) and, recently, cryoablation, have evolved as cornerstone AF ablation techniques. However, a large proportion of patients will still present with AF recurrences within a few years after ablation (1), underscoring the need for a better selection of AF ablation candidates. Thus, efforts to define predictors of AF ablation recurrences have been undertaken.

Late-gadolinium-enhancement cardiac magnetic resonance (LGE-CMR) imaging has been recently proposed to characterize left atrial (LA) anatomy and structural remodeling. LGE-CMR allows quantification of LA volume, shape (including the spherical remodeling) (2), location and extent of pre-ablation (3), and ablation-induced LA fibrosis (4). In general, a more profound atrial remodeling has been shown to predict worse outcomes after ablation procedures: patients with high LA scar burden (5), increased LA sphericity (2) and LA volume, and incomplete ablation lines,(4) have increased AF recurrence risk. In order to allow widespread clinical application of these parameters, a thorough description of the intra- and inter-observer reproducibility and agreement of LGE-CMR measurements is needed. Also, the impact of observers experience on the measurement reproducibility and agreement needs to be assessed.

The aims of this study were: 1). to provide a comprehensive assessment of intra- and inter-observer reproducibility and agreement of LGE-CMR parameters with direct application to AF ablation techniques; 2). to assess the impact of observer experience on the reproducibility and agreement of these measurements.

Methods.

Patients

This work was performed in LGE-CMR data collected as part of the ALICIA (AiLlament de venes pulmonares amb imatge de ressonanCIA - Isolation of pulmonary veins with magnetic resonance imaging; ClinicalTrials.gov: NCT02698631). The study protocol was approved by our hospital's ethics committee, and all participants signed written informed consent.

In short, the ALICIA study was designed to assess the role of documenting the presence of LA fibrosis in guiding AF ablation. All patients recruited in this study had a LGE-CMR examination performed before AF ablation (to assess native LA fibrosis), and a follow-up LGE-CMR study performed 3 months after ablation (to assess ablation-induced LA fibrosis). From all the LGE-CMR examinations performed between October 2015 and February 2017 we randomly selected 20 pre-, and 20 post-ablation LGE-CMR with good or excellent image quality (according to visual assessment performed by an expert technician). Data were anonymized and transferred into a secured off-line server.

LGE-CMR acquisition

The acquisition protocol has been previously reported (4,6). Briefly, images were acquired 20 min after an intravenous bolus injection of 0.2 mmol/kg gadobutrol (Gadovist, BayerShering) using either a 1.5 or a 3-Tesla magnetic resonance scanner (Magnetom Trio, Siemens Healthcare), and an ECG-gated sequence with respiratory navigator. Inversion time was set to suppress the healthy left ventricle myocardium.

Analysis of the LGE-CMR

Post-processing of the LGE-CMR data was performed using the ADAS-AF software (Galgo Medical S.L., Barcelona, Spain). Delineation of LA myocardium was

achieved by manually tracking the mid-wall of the LA in each transverse LGE-CMR slice plane. The software then generated a 3D model of the LA from the slice-by-slice segmentation. The 3D reconstruction and the correctness of LA wall tracking was then checked by the operator and manually adjusted as necessary. On the final 3D model of the LA, the ADAS-AF software maps the LA fibrosis based on individual voxel intensity. The ADAS-AF color map allocates blue for healthy tissue, white for areas with increasing fibrosis density, and red for dense scar fibrotic areas. We used previously validated intensity threshold values for healthy and dense scar tissue (6). Briefly, the IIR (image intensity ratio) was calculated as the ratio between the voxel intensity of the LA myocardium to the average and normalized intensity of the LA blood pool (7). An $IIR \geq 1.20$ identified atrial fibrosis, while an $IIR > 1.32$ was considered dense fibrotic tissue. An illustrative example of the analysis of the LGE-CMR images is presented in Figure 1.

Reproducibility and agreement study protocol

Three experienced and 3 non-experienced observers were selected for this work. Experienced observers were defined as those with >12 months experience in LGE-CMR analysis, and who had performed >100 LGE-CMR segmentations and interpretations. Non-experienced observers were defined as those with <3 months experience in LGE-CMR analysis and <20 LGE-CMR analysis performed prior to this study. Every observer was given raw MR images, and was requested to conduct the whole procedure, including image segmentation, pulmonary veins (PV), mitral valve (MV) and LA appendage (LAA) exclusion, and fibrosis quantification.

Before commencing this study, all non-experienced observers followed a brief training consisting in performing 10 LGE-CMR segmentation and interpretations (5

pre-, and 5 post-ablation) under direct supervision of an experienced observer. In addition, joint review sessions were held to ensure that each observer conducted LGE-CMR analyses in a similar way. All observers were blinded to the patients' clinical data (including AF type: paroxysmal vs. persistent, and LGE-CMR data: pre- or post-ablation).

Intra-observer reproducibility and agreement.

One experienced (FA) and 1 non-experienced (ADM) observer performed complete LGE-CMR data analysis in all 40 patients, twice, in different days.

Inter-observer reproducibility and agreement.

Two experienced observers (EB, FC) and 2 non-experienced (NE, JC) performed complete LGE-CMR data analysis in a subgroup of 30 patients (15 pre-ablation, and 15 post-ablation LGE-CMR), once. The use of multiple observers for inter-observer reproducibility and agreement allows for better assessment of measurement variability.

Global LA shape parameters and scar quantification

Each observer measured the following parameters, on the 3D LA model with the PV, LAA, and MV excluded:

- LA volume (ml);
- LA area (cm²), defined as the total LA wall surface area;
- Sphericity index (SI), which evaluates the variation between the LA and the sphere that best fitted the LA shape (2).

- LA scar percentage area (Scar%), defined as the ratio between the total scar area (using a IIR threshold of >1.2) and LA area, x100;
- LA dense scar area (Core%), defined as the ratio between the total dense scar area (using a IIR threshold of >1.32) and LA area, x100;

Pair-wise similarity of 3D models.

Agreement between 3D models was quantified as follows. The PVs, LAA and MV were semi-automatically clipped from each 3D LA model. LA shape differences were analyzed by computing the mean and maximal surface to surface distance between paired 3D LA models. Scar overlap was quantified between each pair of 3D models. We used customized code (Python, VTK) to compute all 3D measurements (See Supplemental Methods and Supplemental Figure 1).

Statistical analysis.

Reproducibility of quantitative data was expressed both with interclass correlation coefficient (ICC) and coefficient of variation (CV). The CV was calculated using the formula:

$$CV = SD/(\text{arithmetic mean of measurements}) \times 100,$$

where SD is the standard deviation of the measurement error associated with a single measurement, calculated as the SD of residuals (measurement 1 – measurement 2) divided by $\sqrt{2}$.

Each pair of observations was compared using a Bland–Altman analysis to estimate the systematic differences between observers (8). Because we used 3 observers for inter-observer reproducibility, pooled results are reported as the mean difference in measurements observed in the comparisons between all 3 pairs of observers.

Congruency of 3D model was assessed by measuring the maximal and the average distance between each closest pair of LA surface points.

Scar overlap was assessed using the Dice coefficient (which takes values from 0 – no scar overlap, to 1 – perfect scar overlap) (9), and total agreement (%) between the healthy and scarred LA areas.

Results.

Baseline characteristics of the study population are displayed in Table 1.

Reproducibility global LA shape parameters and scar quantification

Both intra- and inter-observer reproducibility of LA volume, LA area, and SI were good (CV <10%, ICC >0.71), regardless of observer's experience (Table 2). Intra-observer reproducibility of scar extension was also good (CV <12.1%; ICC >0.98), regardless of observer's experience or whether the LGE-CMR was performed pre- or post-ablation. However, inter-observer CVs of scar extension were only moderate in pre-ablation LGE-CMR, but remained good in post-ablation LGE-CMR; the ICC remained good (>0.97) (Table 2). Corresponding intra- and inter-observer correlation and Bland-Altman graphs are presented in Supplementary Figure 2.

Congruency of 3D model

The 3D model reconstruction was highly congruent, yielding a mean difference between 3D shells of less than 1 mm in all cases (Figure 2A, 2B). The maximal error between shells was found to be less than 4.6 mm for intra-observer reproducibility analyses, and less than 7 mm for inter-observer analyses; these were mainly located at the posterior aspect of the LAA and at the left PV ostia (Figure 3).

Scar overlap

Overall, location of scar had acceptable intra-observer and inter-observer overlap. Also, the agreement between healthy and scar tissue location was very good (Figure 2C). The relationship between scar burden (Scar%) and precision of overlap (Dice coefficient) is depicted in Figure 4. For intra-observer reproducibility assessment, scar overlap between repeated segmentations was good (Dice coefficient >0.75) for scar areas $>5 \text{ cm}^2$. However, good scar overlap between different observers occurred for larger scars ($>15 \text{ cm}^2$). Because scar burden increased after the ablation procedure, scar overlap between and within observers appears lower in pre-ablation compared with post-ablation LGE-CMRs. However, as displayed in Figure 4, the precision of scar overlap depends mostly on scar extension. The experience of the observers had no influence on scar location ($p = \text{NS}$ for all comparisons between experienced and non-experienced observers). An example of scar overlap between observers is given in Figure 5.

Discussion.

This is the most comprehensive study of the reproducibility and agreement of LGE-CMR parameters when used for LA fibrosis assessment, before and after AF ablation procedures. Our findings can be summarized as follows: 1. LGE-CMR measurements of LA area, volume and SI are highly reproducible; 2. Geometric congruency of LA shape is high, with maximal error $<5\text{mm}$ for intra-observer and $<8\text{mm}$ for inter-observer repeated measurements; 3. Precision of scar location increases with extent of scar, and is good when the scar area is $>5\text{cm}^2$ for a single observer, and $>15 \text{ cm}^2$ for multiple observers; 4. Non-experienced observers performed equally well

to experienced observers. As a result, LGE-CMR assessment of LA measurements and scar extension can be applied in clinical practice after minimal training.

Few studies have assessed the reproducibility of LGE-CMR detected LA fibrosis, and none specifically addressed the impact of observer's experience on reproducibility, nor did they assessed the accuracy of scar overlap or geometric congruency of the reconstructed 3D shell (10). Also, most of studies used the Corview software package and the DECAFF protocol to detect and quantify LA fibrosis (10). The inter-observer ICC reported for quantification of LA fibrosis was good in all studies in both paroxysmal and persistent AF (ICC >0.79) (11-13). We have also reported excellent inter-observer ICC for detecting LA fibrosis,(6) and measuring the SI (ICC >0.94 for both) (2) using the GIMIAS software (a previous version of ADAS). Defining the reproducibility of LGE-CMR parameters for AF ablation is important if LA fibrosis assessment is to be introduced in clinical practice in order to improve outcomes. For example, research is underway to identify an optimized ablation strategy in patients undergoing AF radiofrequency ablation on the basis of left atrium (LA) fibrosis characterization (the ALICIA study, ClinicalTrials.gov: NCT02698631). Scarred LA areas (as defined by LGE-CMR) can be used as bridges between ablation lesions, thus potentially shortening the duration of the procedure, increasing safety, without compromising efficacy. Also, in redo procedures, only gaps in ablation lines may be targeted. Our results provide important data in this respect, by defining the reproducibility of scar overlap assessment in relation to the scar dimension. The precision of scar delimitation becomes low only in patients with scar areas <5 cm² (or ~5% of LA area – so called UTAH class I LA fibrosis classification) – but this amount of LGE-CMR-defined fibrosis is frequently seen in healthy individuals (6). However, it is unlikely that in this group of patients defining the exact location and extent of scar

patches will change the ablation strategy, and a complete PVI will still be necessary.

When multiple observers are involved in analyzing LGE-CMR images, however, high precision of scar delineation can be achieved for scar areas $>15 \text{ cm}^2$, so scar location for UTAH I and II LA fibrosis classification (scar area up to 20% of LA area) will may be inadequately defined (14). Thus, efforts to improve LGE-CMR reproducibility of LA fibrosis assessment are still warranted. Automatic segmentation algorithms are likely to achieve this goal, and are currently under development.

Limitations.

We did not assess the impact of repeated LGE-CMR acquisition on LGE-CMR measurements (especially on precision of scar location) by single and different observers (true test-retest reproducibility). These data would be important, but such studies are difficult to be carried out in clinical settings, especially in LGE-CMR. Also, by protocol, we only selected for analysis good quality LGE-CMR images, so we did not report on the feasibility of LGE-CMR assessment of LA fibrosis; about one quarter of studies were excluded due to poor LGE-CMR image quality.

Conclusions.

LGE-CMR measurements of LA area, volume and SI are highly reproducible, and geometric congruency of LA shape is high. Location of scar is highly precise for scar areas $>5 \text{ cm}^2$ for single observers and $>15 \text{ cm}^2$ for multiple observers. LGE-CMR assessment of LA measurements and scar extension can be applied in clinical practice after minimal training.

Clinical competencies.

The results of this study are important for the procedural skills of technicians and doctors involved in LGE-CMR evaluation of left atrial fibrosis for AF ablation and, subsequently, for patients' care. Measurements of LA size and shape are highly reproducible. The precision of scar location is high when the scar area was $>5\text{cm}^2$ (intra-observer), and $>15\text{ cm}^2$ (inter-observer). LGE-CMR assessment of LA measurements and scar extension may be applied in clinical practice after minimal training.

Translational outlook.

This study defines the reproducibility of LGE-CMR measurements on already acquired images. Future studies should identify highly reproducible LGE-CMR indices that are simple to measure, and are major predictors of AF ablation success. Detailed studies should be performed regarding the impact of acquisition and measurement reproducibility on diagnostic accuracy, treatment outcome, and cost-efficiency of therapies initiated or continued based on imaging results.

References.

1. Kirchhof P, Benussi S, Kotecha D, et al.; ESC Scientific Document Group. 2016 ESC Guidelines for the management of atrial fibrillation developed in collaboration with EACTS. *Eur Heart J*. 2016;37:2893-62.
2. Bisbal F, Guiu E, Calvo N, et al. Left atrial sphericity: a new method to assess atrial remodeling. Impact on the outcome of atrial fibrillation ablation. *J Cardiovasc Electrophysiol*. 2013;24:752-9.
3. Benito EM, Cabanelas N, Nuñez-Garcia M, et al. Preferential regional distribution of atrial fibrosis in posterior wall around left inferior pulmonary vein as identified by late gadolinium enhancement cardiac magnetic resonance in patients with atrial fibrillation. *Europace*. 2018 May 31. doi: 10.1093/europace/euy095. [Epub ahead of print]
4. Bisbal F, Guiu E, Cabanas-Grandío P, et al. CMR-guided approach to localize and ablate gaps in repeat AF ablation procedure. *JACC Cardiovasc Imaging*. 2014;7:653-63.
5. Marrouche NF, Wilber D, Hindricks G, et al. Association of atrial tissue fibrosis identified by delayed enhancement MRI and atrial fibrillation catheter ablation: the DECAAF study. *JAMA*. 2014;311:498-506. Erratum in: *JAMA*. 2014;312:1805.
6. Benito EM, Carlosena-Remirez A, Guasch E, et al. Left atrial fibrosis quantification by late gadolinium-enhanced magnetic resonance: a new method to standardize the thresholds for reproducibility. *Europace*. 2017;19:1272-9.
7. Khurram IM, Beinart R, Zipunnikov V, et al. Magnetic resonance image intensity ratio, a normalized measure to enable interpatient comparability of left atrial fibrosis. *Heart Rhythm*. 2014;11:85-92.

8. Bland JM, Altman DG. Statistical methods for assessing agreement between two methods of clinical measurement. *Lancet*. 1986;1(8476):307-10.
9. Zou KH, Warfield SK, Bharatha A, et al. Statistical validation of image segmentation quality based on a spatial overlap index. *Acad Radiol*. 2004;11:178-89.
10. Siebermair J, Kholmovski EG, Marrouche N. Assessment of left atrial fibrosis by late gadolinium enhancement magnetic resonance imaging: methodology and clinical implications. *JACC Clin Electrophysiol*. 2017;3:791-802.
11. Akoum N, Fernandez G, Wilson B, McGann C, Kholmovski E, Marrouche N. Association of atrial fibrosis quantified using LGE-CMR with atrial appendage thrombus and spontaneous contrast on transesophageal echocardiography in patients with atrial fibrillation. *J Cardiovasc Electrophysiol*. 2013;24:1104-9.
12. Cochet H, Mouries A, Nivet H, et al. Age, atrial fibrillation, and structural heart disease are the main determinants of left atrial fibrosis detected by delayed-enhanced magnetic resonance imaging in a general cardiology population. *J Cardiovasc Electrophysiol*. 2015;26:484-92.
13. McGann C, Akoum N, Patel A, et al. Atrial fibrillation ablation outcome is predicted by left atrial remodeling on MRI. *Circ Arrhythm Electrophysiol*. 2014;7:23-30.
14. Akoum N, Daccarett M, McGann C, et al. Atrial fibrosis helps select the appropriate patient and strategy in catheter ablation of atrial fibrillation: a DE-MRI guided approach. *J Cardiovasc Electrophysiol*. 2011;22:16-22.

Table 1. Baseline characteristics of the study population.

	Total	Pre-ablation N = 20	Post-ablation N = 20	P value
Demographic characteristics				
Age (years)	60.0 ± 12.8	60.1 ± 13.5	59.9 ± 12.3	0.98
Men (n, %)	26 (65)	12 (60)	14 (70)	0.37
Paroxysmal AF (n, %)	24 (60)	15 (75)	9 (45)	0.10
CMR characteristics				
LA volume (ml)	81.7 ± 27.0	81.1 ± 23.9	82.3 ± 30.1	0.89
LA area (cm²)	88.4 ± 19.1	89.5 ± 17.1	87.4 ± 21.0	0.73
Sphericity Index	78.8 ± 4.1	77.6 ± 3.8	80.0 ± 4.1	0.008
Scar (%)	17.3 ± 16.3	9.3 ± 13.7	25.3 ± 14.9	<0.001
Core (%)	9.3 ± 11.9	3.8 ± 8.7	14.7 ± 12.3	<0.001

Note: CMR, cardiac magnetic resonance; LA, left atrium

Table 2. Reproducibility of quantitative LGE-CMR parameters.

	TOTAL		Pre-ablation		Post-ablation	
	ICC	CV%	ICC	CV%	ICC	CV%
Experienced						
Intra-observer						
LA volume	0.983	4.2	0.981	3.6	0.988	4.0
LA area	0.953	4.1	0.934	4.0	0.977	3.4
SI	0.923	1.5	0.848	2.1	0.983	0.7
Scar%	0.991	9.0	0.997	8.2	0.983	7.7
Core%	0.993	10.8	0.999	8.8	0.987	9.1
Inter-observer						
LA volume	0.972	5.1 ± 0.4	0.975	4.5 ± 0.3	0.972	5.6 ± 0.8
LA area	0.786	7.9 ± 4.8	0.884	5.6 ± 3.4	0.711	9.5 ± 5.7
SI	0.818	2.3 ± 0.7	0.829	1.9 ± 0.3	0.799	2.5 ± 1.1
Scar%	0.983	12.0 ± 2.8	0.983	19.2 ± 5.1	0.975	9.2 ± 2.3
Core%	0.981	16.8 ± 3.9	0.977	28.2 ± 16.6	0.976	12.4 ± 2.7
Non-experienced						
Intra-observer						
LA volume	0.984	4.2	0.979	4.3	0.990	3.7
LA area	0.955	4.5	0.954	4.2	0.963	4.6
SI	0.977	0.8	0.985	0.6	0.969	0.9
Scar%	0.996	6.2	0.993	12.1	0.996	3.7
Core%	0.997	7.6	0.998	9.6	0.995	6.0
Inter-observer						
LA volume	0.964	5.9 ± 1.0	0.953	6.3 ± 1.8	0.979	5.5 ± 1.0
LA area	0.904	6.6 ± 1.0	0.885	7.1 ± 1.9	0.934	5.5 ± 1.0
SI	0.889	1.5 ± 0.5	0.892	2.4 ± 2.2	0.880	1.6 ± 0.4
Scar%	0.985	11.8 ± 3.2	0.990	13.9 ± 4.4	0.978	8.7 ± 2.2
Core%	0.989	14.1 ± 4.0	0.981	18.5 ± 5.3	0.990	9.3 ± 3.0

Figure Legends.

Figure 1. Example of LGE-CMR image segmentation and analysis.

The sequence of defining scar areas on late gadolinium enhanced cardiac magnetic resonance imaging (LGE-CMR) using the ADAS-AF program. First, LGE-CMR images were acquired using a standardized protocol and were imported into the ADAS-AF program (**A**). The left atrial wall was tracked manually at different levels, and the program used those boundaries to define the blood pool intensity based on voxel intensity (**B**), and reconstructed a provisional 3D shape of the left atrium (**C**). The operator checked the accuracy of wall tracking on every slide, and a final 3D left atrial geometry was created (**D**). Then, the software projected the intensity value of the LGE-CMR to each voxel of the 3D model (**E**), and displayed this information as a colour map (i.e. representing fibrosis) superimposed on the 3D volume (**F**). Finally, the pulmonary veins, left atrial appendage, and mitral valve were excluded from the model (**G**).

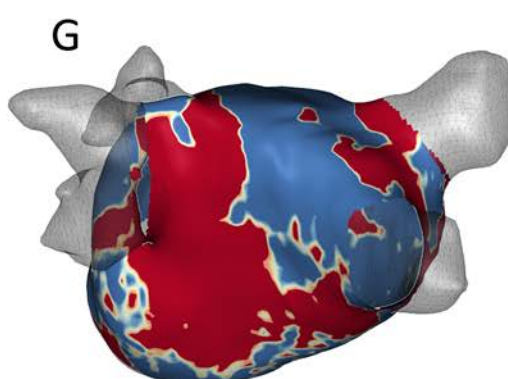
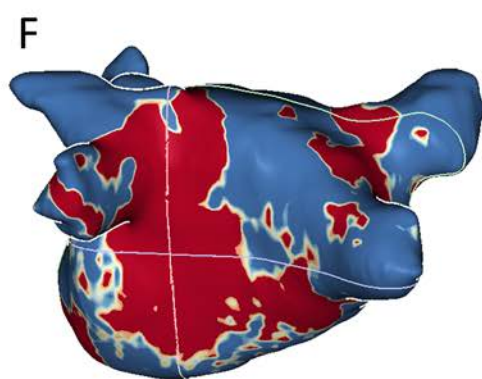
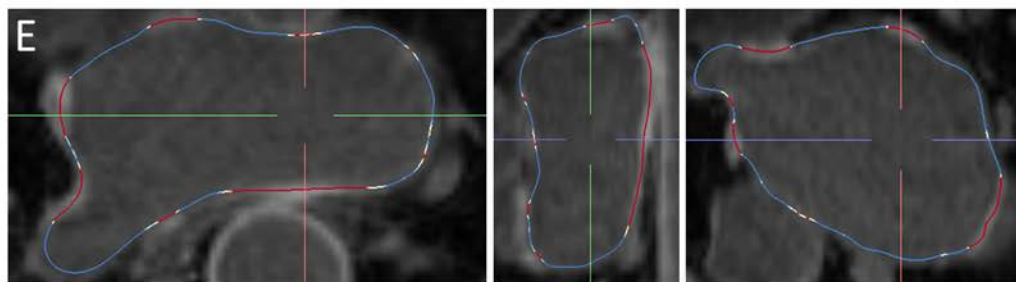
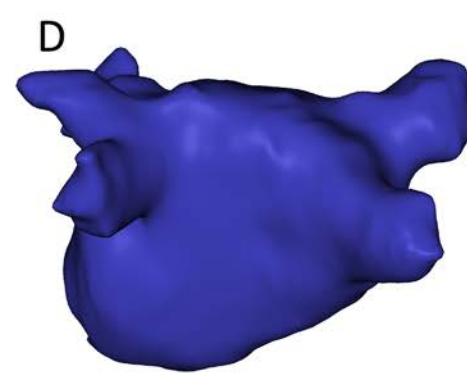
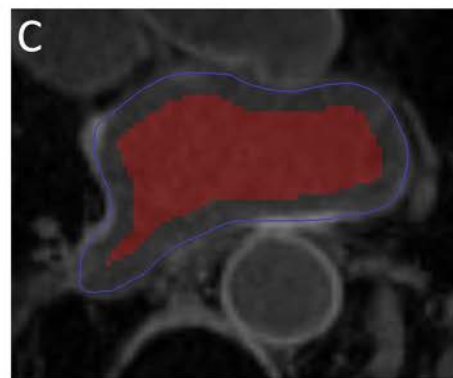
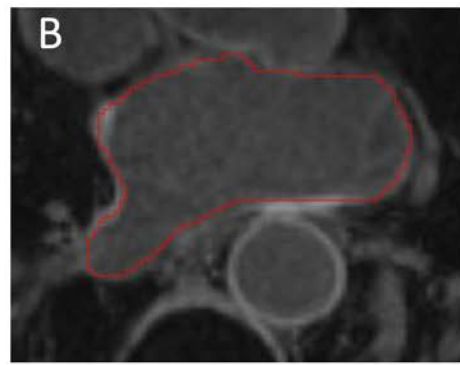
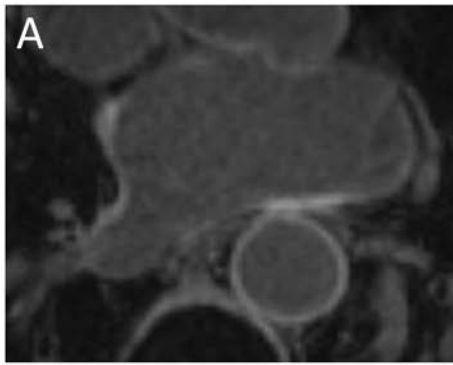


Figure 2. Congruency of LA 3D model (mean and maximal surface-to-surface distance between 3D shells) (**A,B**), and precision of scar overlap (Dice coefficient) (**C**).

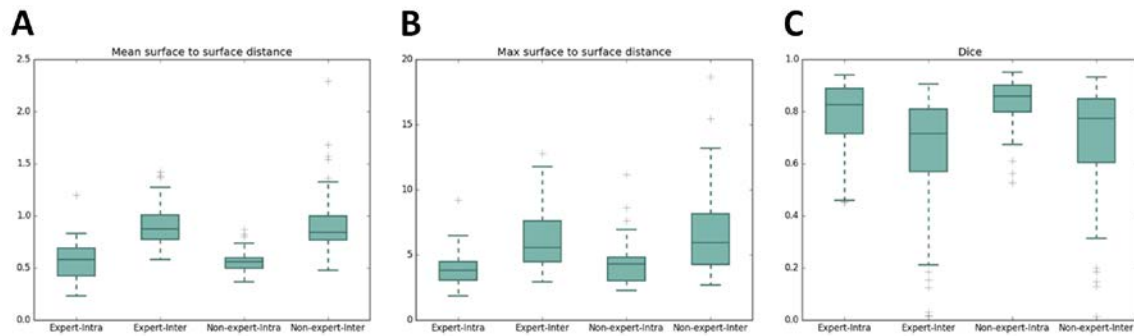


Figure 3. Example of geometric errors between observers in reconstructed 3D left atrial shapes.

A posterior view of the left atrium is depicted where a pair of 3D reconstructions of the left atrium (named S and T - each performed by different observers) is projected one to the other. The left image depicts the color-coded maximal distance between the 3D shapes, when one shape (S) is used as reference and the other shape (T) is forced to project to it. The right image depicts the opposite analysis (shape T used as reference, while shape S is projected to shape T). The color map indicates surface to surface distance ranging from 0 (green) to the maximum distance between the surfaces (red). In this example, the maximal error occurs around the left and right pulmonary vein ostia.

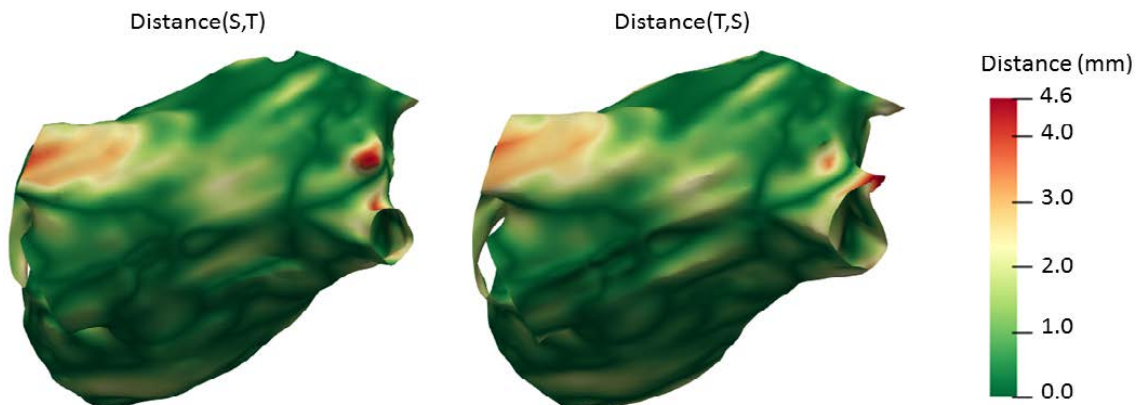


Figure 4. Precision of overlap of scar assessment by cardiac magnetic imaging (using Dice coefficient) in relation to scar area, in experienced and non-experienced operators.

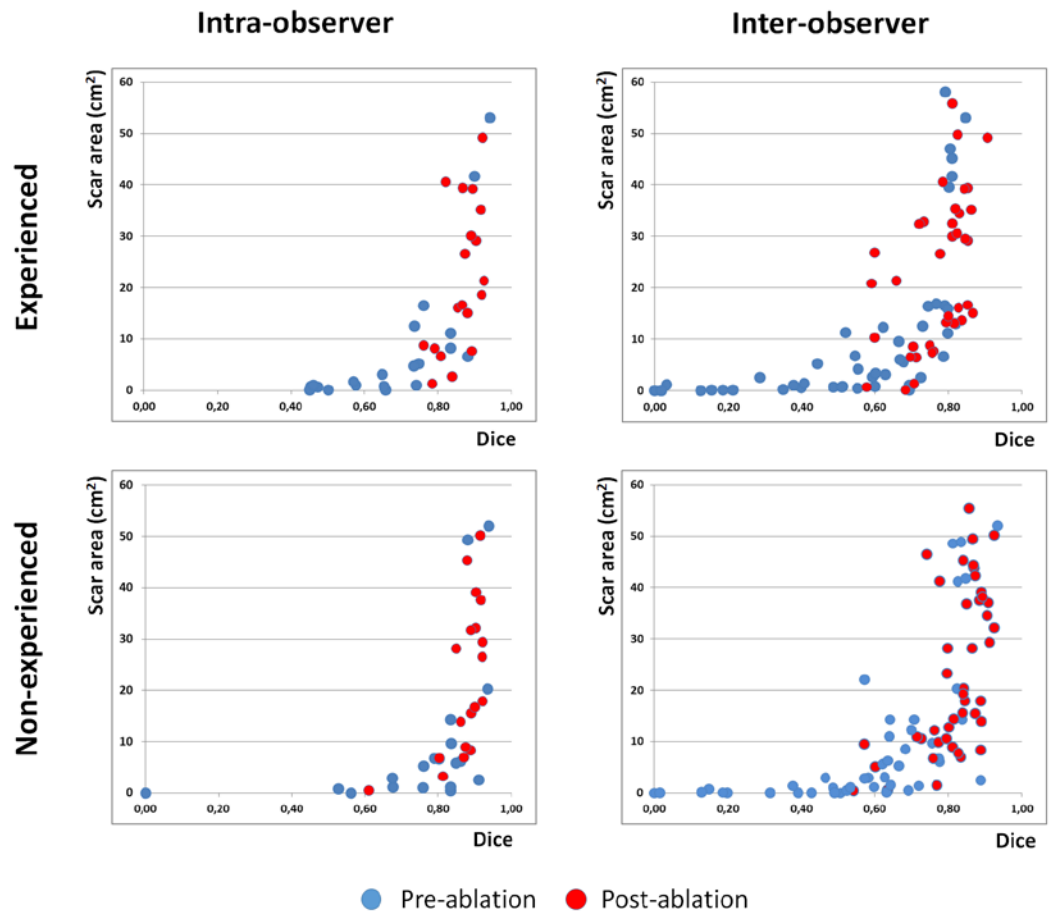


Figure 5. Example of pair-wise scar overlap measurements for a given LGE-CMR image, for experienced (A) and non-experienced (B) observers. The initials of the observer performing the segmentation is displayed above each image, and the Dice coefficient of paired comparison below overlapped scar projections.

